



RESEARCH ARTICLE

STUDY OF THE ADSORBER-COLLECTOR PERFORMANCE OF A SOLAR ADSORPTION COOLING UNIT USING THE ZEOLITE-WATER PAIR AND OPERATING UNDER THE DRY TROPICAL CLIMATIC CONDITIONS

\* Hassime GUENGANE, Amadou KONFE, Abdoulaye COMPAORE, Sié KAM, S.M. Thierry KY and D. Joseph BATHIEBO

Laboratory of Renewable Thermal Energies (LETRE), Université Ouaga 1 Pr. Joseph KI-ZERBO, BP 7021 Burkina Faso, West Africa

ARTICLE INFO

Article History:

Received 18<sup>th</sup> March, 2018  
Received in revised form  
23<sup>rd</sup> April, 2018  
Accepted 29<sup>th</sup> May, 2018  
Published online 30<sup>th</sup> June, 2018

Key words:

Solar Refrigeration, Zeolite-Water pair, Adsorption phenomenon, Solar Performance Coefficient, Cooling Capacity.

\*Corresponding author

Copyright © 2018, Hassime GUENGANE et al. This is an open access article distributed under the Creative Commons Attribution License, which permits unrestricted use, distribution, and reproduction in any medium, provided the original work is properly cited.

Citation: Hassime GUENGANE, Amadou KONFE, Abdoulaye COMPAORE, Sié KAM, S.M. Thierry KY and D. Joseph BATHIEBO. 2018. "Study of the adsorber-collector performance of a solar adsorption cooling unit using the zeolite-water pair and operating under the dry tropical climatic conditions..", *International Journal of Current Research*, 10, (06), 70483-70494.

ABSTRACT

In this paper we present the distribution of simulated state variables in a -adsorber-collector prototype of an adsorption solar refrigerator designed to work with the zeolite-water pair under the climatic conditions of the city of Ouagadougou. The solar performance factor (COPs) and the cooling capacity (SCP) are the parameters studied for evaluating the system performance. The simulation of these quantities is obtained from the heat and mass transfer equilibrium equations, solved by a numerical scheme using Thomas' algorithm (TDMA). The Dubinin-Astakhov adsorption model is used to model the adsorption phenomenon. A MATLAB program has been developed for the numerical simulation of the problem. In order to get closer to the local operating conditions, we have implemented in the MATLAB program, values of the sunshine, the wind speed and the ambient temperature recorded on the IRSAT solar adsorption refrigerator collector during four successive days of April of the year 2016. For a zeolite mass of 10 kg, and for the condensation and evaporation temperatures set respectively at  $T_c = 30^{\circ}C$  and  $T_e = 5^{\circ}C$ , we found the COPs and the SCP varying respectively from 0.094 to 0.10 and from  $0.6834 \times 10^3 MJ$  to  $10.0017 \times 10^3 MJ$ .

INTRODUCTION

In Burkina Faso as in developing countries, the requirement of cooling for the preservation of food and pharmaceuticals is steadily increasing. The energy needed to meet these requirements is largely provided by the National Electricity Company of Burkina (SONABEL). Rural populations outside the coverage areas of the electricity network therefore do not benefit from refrigerating systems. In addition, this energy is of fossil origin (unsafe sources) and cold production devices are conventional compression-refrigerators using greenhouse gases as refrigerants. In this context, for those countries with favorable sunshine, the production of cold by solar energy seems to be a promising way. For solar adsorption refrigerators, producing cold intermittently, the main advantage is the simplicity of their design (no need for spare parts or mechanical intervention) and their total energy autonomy during the cold production phase. In addition, using fluids other than C.F.C., they do not affect the environment. Adsorption solar refrigeration has been studied since the sixties (Trombe, 1956), but it was only towards the end of the seventies that interest in this process grew and led to the conception of prototypes using performances of the adsorbent-refrigerant pairs such as active carbon-methanol (Wassila, 2008; Konfe et al., 2016), zeolite-water (Meunier, 1988; Zoubir, 2007 ; Bing Xue, 2015), activated carbon-ammonia (El Amers, 2002 ; Mimmet, 1991; Al Mers, 20069) and silicagel-water (Konfe Amadou, 2011; Adell, 1984). The adsorber collector is the driving force of these systems. Several studies have been conducted in order to improve its performance and thus improve the performance of the whole system (Wassila, 2008 ; Konfe Amadou, 2017; Adell, 1984; Meunier, 1986; Krache, 1996 Mohammed Abdel, 2002; Lemmin, 1992). This work focuses on the simulation of the adsorber-collector condition variables operating under the climatic conditions of the city of Ouagadougou with a view to optimizing the performance of the system.

## Classifications

$T_v$	Glass Temperature ( $^{\circ}\text{C}$ )
$T_{\text{abs}}$	Adsorber temperature ( $^{\circ}\text{C}$ )
$T_c$	Condenser temperature ( $^{\circ}\text{C}$ )
$T_e$	Temperature of the evaporator ( $^{\circ}\text{C}$ )
$T_a$	Ambient temperature ( $^{\circ}\text{C}$ )
$T_{\text{amb}}$	Maximum ambient temperature ( $^{\circ}\text{C}$ )
$T_{\text{HLS}}$	Ambient temperature of sunrise ( $^{\circ}\text{C}$ )
$P_{\text{sat}}(T)$	saturation pressure at temperature $T$ (Pa)
$\lambda_{\text{eq}}$	Equivalent thermal conductivity of adsorbate ( $\text{W}/\text{m}^2\text{ }^{\circ}\text{C}$ )
$C_{\text{pt}}$	Specific heat of adsorbate ( $\text{kJ}/\text{kg}^{\circ}\text{C}$ )
$m$	Adsorbed mass of the adsorbate ( $\text{kg}/\text{kg}$ )
$W_0$	Maximum adsorption capacity
$D$	Constant characteristic related to the adsorbent / adsorbate couple
$n$	Exponent of the Dubinin-Astakhov equation adsorbent / adsorbate couple
$\rho_l(T)$	Density of the liquid adsorbate ( $\text{kg}/\text{m}^3$ )
$I_g$	Ig Solar Flash Flux ( $\text{W}/\text{m}^2$ )
$m_a$	Mass of adsorbent ( $\text{kg}/\text{kg}$ )
$m_{\text{pm}}$	Mass of the metal parts of the adsorber ( $\text{kg}$ )
$C_{\text{pm}}$	Specific heat of the metal parts of the adsorber ( $\text{kJ}/\text{kg}^{\circ}\text{C}$ )
$Q_{\text{rost}}$	Isosteric heat (kJ)
$L$	Latent heat of adsorbate ( $\text{kJ}/\text{kg}$ )
HLS	Sunrise time
HCS	Sunset time
$\text{COP}_S$	Solar Performance Coefficient
$Q_{\text{evapo}}$	Quantity of cold drawn off at the evaporator (kJ)
$G_{\text{tot}}$	incident solar energy (kJ)
SCP	Cooling capacity (W)

## Description of the system

**Ideal operating cycle of an adsorption solar fridge :** When connecting an adsorber collector in which an adsorbent containing a refrigerant is trapped to a condenser and an evaporator, an adsorption cooling cycle is carried out. The ideal cycle thus produced follows the principle of reversibility of the adsorption. It can be represented by the Clapeyron thermodynamic diagram ( $\ln P = f(-1/T)$ ) as shown in Figure 1.

Fig. 1. Ideal operating cycle of an adsorption solar refrigerator (Phillipe, 2015)

Phase	Description	Schematic	Diagram
1. Isosteric heating (7h-10h)	The sunshine received by the collector causes both the increase of the temperature and of the pressure of the system until reaching the saturation pressure corresponding to the condensation temperature; the concentration of the refrigerant remaining constant.		
2. Isobaric heating: desorption and condensation (14h-16h)	As the adsorber heater continues, the refrigerant is desorbed as vapor. This desorption is done at constant pressure until the temperature of the system reaches its maximum value. The water vapor condenses in the condenser and flows to the evaporator.		
3. Isosteric cooling (16h-19h)	The cooling of the collector is related to the decrease of sunshine. The pressure of the system decreases to reach the pressure of the evaporator.		
4. Isobaric cooling: adsorption and cold production (19h-7h)	This is the phase during which cold is produced. The pressure and the temperature decrease. The zeolite is in physical imbalance and will "recharge" in water vapor produced by evaporation in the refrigerated enclosure. This evaporation produces the cold by withdrawal of the latent heat of evaporation of the water.		

When the temperature level in the evaporator reaches the freezing point, there is solidification and formation of ice stock.

**Description of the adsorber collector:** There are several models related to the geometry of the adsorbent container. The most developed are tubular or planar adsorbers. The collector prototype that is the subject of our study is a component of an adsorption solar refrigerator developed in the Renewable Thermal Energy Laboratory (LETRE) by a group of Belgian students as part of the MA1 2008/09 project (Delporte Loïc et al., 2008). This prototype is intended for vaccine storage. The sensor is connected alternately to a condenser and an evaporator as shown in figure 2.a) below. This is a box containing a diffuser which consists of a grid arranged in the form of a triangle (figure 2.b and 2.c). In this device, a triangle over two is filled with adsorbent, while the others remain free to allow the passage of water removed from the adsorbent bed during the desorption process. Figure 2.b) shows an exploded view of this model.

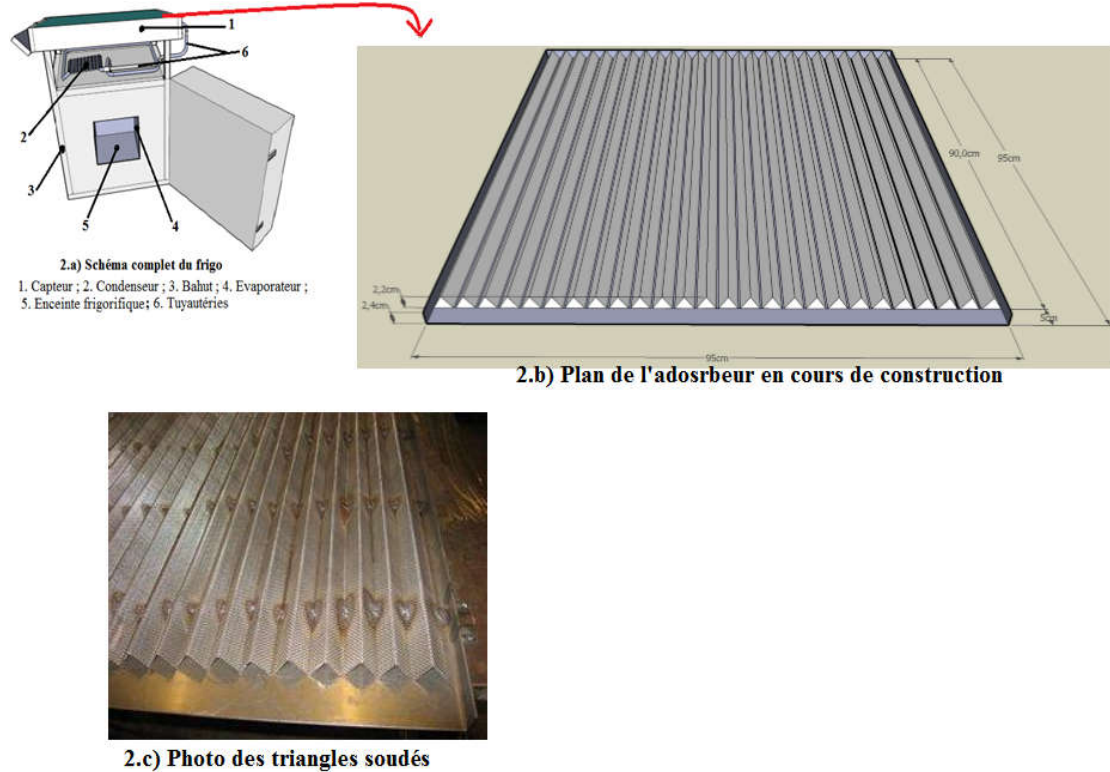


Fig. 2. Schema of the studied model (Delporte Loïc, 2008)

## Mathematical model of the adsorber collector

### Simplifying hypotheses

To simplify the equations governing the process of heat and mass transfer in each triangular diffuser, we will consider that:

- The inertia of the adsorber is negligible
- The temperature ( $T_v$ ) range of the glass cover is uniform.
- The cover is opaque to infrared radiation.
- The cover and the adsorber are supposed to be gray bodies in the meantime
- ( $0\mu\text{m}$ ,  $3\mu\text{m}$ ) wavelength of solar radiation and in the range  $\lambda > 3\mu\text{m}$  are opaque bodies.
- There is no resistance to mass transfer in the adsorbent bed.
- The physical properties of the metallic parts of the adsorber and the adsorbent are constant with the exception of the adsorbate.
- The reactive medium is a continuous medium characterized by equivalent thermal conductivity  $\lambda_{eq}$ .
- The height of the triangles are such that the temperature field is uniform inside.
- Only heat transfer by conduction is considered in the vapor phase. Convection is negligible because of the low flow rate of the adsorbate.
- The pressure is uniform ( $gradP = 0$ ) but depends on the weather.
- The specific heat of the adsorbed phase is equal to that of the adsorbate liquid ( $C_{pl} = C_{pg}$ ).
- During the desorption-condensation phase, the pressure of the reactive medium is equal to the saturation pressure corresponding to the condensation temperature ( $P = P_{sat}(T_c)$ ). During the adsorption-evaporation phase, the pressure is equal to that of saturation corresponding to the evaporation temperature ( $P = P_{sat}(T_e)$ ).

## Theories of adsorption models

The main models that have successfully treated the adsorption phenomenon and that can explain or interpret it are: the molecular models of Langmuir and Brenauer, Emmett and Teller (BET) (18,19) and thermodynamic ones developed by Polanyi (20, 21, 22) which will be further deepened by Dubinin - Astakhov (23, 24, 25).

In this paper, we will use the mathematical model established by Dubinin-Astakhov to describe the adsorption isotherms. This model results in equation (1) below:

$$m = W_0 \rho_i(T) \exp \left[ -D \left( T \ln \left( \frac{P_{sat}(T)}{P} \right) \right)^n \right] \quad (1)$$

corresponds to the mass of water adsorbed as a function of temperature  $T$  and pressure  $P$ ;  $\rho_i(T)$  and  $P_{sat}(T)$  are respectively the density and the saturation pressure of the water at the temperature  $T$ .  $W_0$  is the maximum adsorption capacity;  $D$  is a constant that characterizes the size and distribution of microspores of the adsorbent and  $n$  is a parameter related to the heterogeneity of the adsorbent.  $D$  and  $n$  therefore depend on the adsorbent / adsorbate pair used. For the zeolite-water pair,  $\rho_i(T)$  and  $P_{sat}(T)$  are respectively calculated from relations (2) and (3) below (Leite, 2000):

$$\rho_i(T) = 667.4 + 2.8367T - 6.9853 \times 10^{-3}T^2 + 3.9556 \times 10^{-3}T^3 \quad (2)$$

$$\ln P_{sat}(T) = 7.924966 - \frac{103979.9}{T} - \frac{103979.9}{T^2} \quad (3)$$

For the adsorption kinetics of the refrigerant particles, we use the (Linear Driving Force-LDF) linear model translated by the equation (4):

$$\frac{\partial m}{\partial t} = k(m^* - m) \quad (4)$$

In this equation,  $m$  is the amount adsorbed in grams (g),  $m^*$  is the amount adsorbed at equilibrium and  $k$  ( $s^{-1}$ ) is the overall kinetic coefficient called LDF coefficient. In the case of an adsorption solar refrigerator where the convective exchanges are not forced, the coefficient  $k$  is calculated from the following relation:

$$k = 15 \frac{D_i}{R_p^2} \quad (5)$$

**Heat transfer balance coupled with mass transfer :** The solar radiation received on the glass face of the collector makes it possible to heat the metallic parts of the collector by greenhouse effect and to raise the temperature and pressure of the adsorbent bed. The temperature and pressure fields are responsible for a mass transfer of the adsorbate in the system. Figure 3 summarizes the heat exchange through the collector.

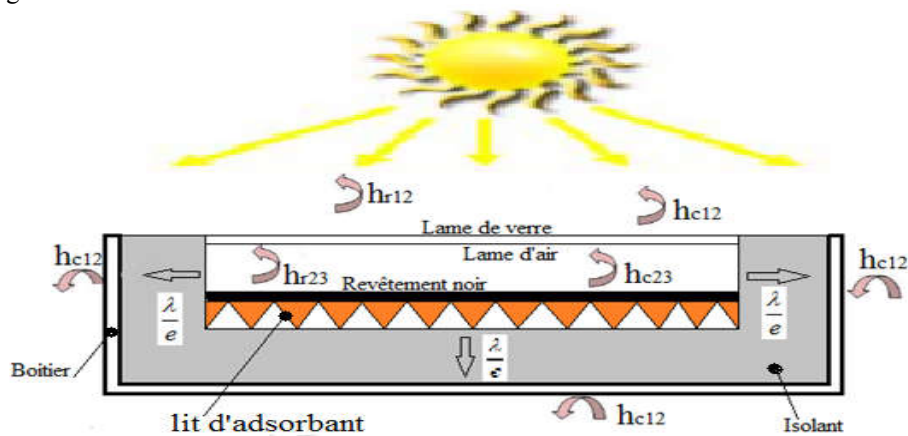


Fig. 3. Thermal exchanges through the collector

**Temperature field and mass transfer in the collector:** Considering the hypotheses mentioned above, the total energy and mass transfer results giving the transient thermal behavior of the solar collector can be written from the system (S) of nonlinear differential equations:

$$(S): \begin{cases} A_1 \frac{dT_v}{dt} = B_1 \times I_g(t) - C_1 \times (T_v - T_a) - D_1 \times (T_{abs} - T_v) \\ A_2 \frac{dT_{abs}}{dt} = B_2 \times I_g(t) - C_2 \times (T_{abs} - T_v) \\ A_3 \frac{dm}{dt} = B_3 - C_3 \frac{dT_{abs}}{dt} \end{cases} \quad (6)$$

The  $A_i$ ,  $B_i$  and  $C_i$  are defined as follows:

$A_1 = m_v C_{pv}$	$B_1 = \alpha_v S_v$	$C_1 = h_{v-atm} S_v$	$D_1 = h_{abs-v} S_v$
$A_2 = m_{pm} C_{pm} + m m_a C_{pl} + m_a C_{pa} + k_p \frac{Q_{isost}^2}{RT_{abs}^2}$	$B_2 = S_{abs} \eta_c$	$C_2 = h_{abs} S_{abs}$	$D_2 = 0$
$A_3 = 1$	$B_3 = nmD(T_{abs})^n \left( \ln \frac{P_{sat}(T_{abs})}{P} \right)^{n-1} \frac{d \ln P}{dt}$ ; $C_3 = nmDT_{abs}^n \left( \ln \frac{P_{sat}(T_{abs})}{P} \right)^{n-1} \frac{Q_{isost}^2}{RT_{abs}^2}$		$D_3 = 0$

$m_{pm}$  corresponds to the mass of the metal parts of the absorber ;  $C_{pm}$  is the specific heat of the metal parts of the absorber ;  $m_a$  is the mass of the adsorbent;  $C_{pa}$  is the specific heat of the adsorbent ;  $C_{pl}$  is the specific heat of the adsorbate;  $T_a$  (K), is the ambient temperature ;  $T_v$  (K), is the temperature of the glass ;  $S_v$  (m<sup>2</sup>), the surface of the glass.  $h_{v-atm}$  (W/m<sup>2</sup>K), the overall exchange coefficient between the glass and the atmosphere is given by (Lemmin, 1992):

$$h_{v-atm} = 5.7 + 3.8 \times V_{vent} + \varepsilon_v \sigma (T_v + T_a)(T_v^2 + T_a^2) \quad (7)$$

$$h_{abs-v} = N_u \left( \frac{\lambda_a}{d} \right) + \sigma \frac{(T_v + T_{abs})(T_v^2 + T_{abs}^2)}{\frac{1}{\varepsilon_v} + \frac{1}{\varepsilon_{abs}} - 1} \quad (8)$$

Where,  $h_{abs-v}$  (W/m<sup>2</sup>K) is the heat exchange coefficient between the glass and the adsorber. In this expression, the Nusselt number  $N_u$  is given by the relation:

$$N_u = 1 + 1.44 \times \left( 1 - \frac{1708 (\sin(1.8\varpi))}{R_a \cos \varpi} \right) \left( 1 - \frac{1708}{R_a \cos \varpi} \right)^* + \left( \left( \frac{R_a \cos \varpi}{5830} \right)^{1/3} - 1 \right)^* \quad (9)$$

where  $R_a$  denotes the number of Raleigh:

$$R_a = \frac{g \beta (T_{abs} - T_v) P_r d^3}{\nu^2} \quad (10)$$

$I_g$  corresponds to the instantaneous irradiation received by the plate during a day ;  $\eta_c$  represents the efficiency of the solar collector and is calculated from the linear relation proposed by (Hilbrand et al., 2004):

$$\eta_c = \eta_0 - \theta \frac{T_{abs} - T_{atm}}{I_g} \quad (11)$$

$\eta_0$  is the optical efficiency of the collector and  $\theta$  corresponds to the overall loss coefficient of the collector on the lateral, front and rear faces. (Konfe Amadou, 2017)

We will take  $\eta_0 = 0.75$  et  $\theta = 0.043$   $Q_{isost}$  isosteric heat.

$$Q_{isost} = L + RT \left( \ln \frac{P_{sat}}{P} \right) + \frac{RT \alpha}{nD} \left( T \ln \frac{P_{sat}}{P} \right)^{1-n} \quad (12)$$

$$\alpha = \frac{d\rho_i(T)}{dT}, \quad L = RT^2 \left( \frac{d \ln P_s}{dT} \right)$$

**Boundary conditions :** At the beginning of the cycle, we assume that the solar reactor is in thermal equilibrium with the ambient environment. As a result, the initial values of temperature, pressure and mass are defined as follows:

- $T_v(t=0) = T_{abs}(t=0) = T_a(t=HLS)$ , HLS= sunrise time ;
- $P(t=0) = P_{sat}(T_e) = P_e$ , is the saturation pressure at the evaporation temperature  $T_e$ .
- $m = m(T_a(t=HLS), P_e)$  is the amount of adsorbate trapped in the adsorbent bed at room temperature.

#### 4. Evaluation of solar performance coefficient and cooling capacity

##### Solar Performance Coefficient $COP_s$

The solar coefficient of performance  $COP_s$  of a solar adsorption refrigeration system is the ratio between the amount of cold drawn off at the evaporator  $Q_{evapo}$  and the total solar energy incident during daily illumination  $G_{tot}$ .

$$COP_s = \frac{Q_{evapo}}{G_{tot}} \quad (13)$$

With:

$$Q_{evapo} = 1000 + 0.095G_{tot} - 18T_{amb} - 53T_{HLS} \quad (\text{Boubakri et al., 1992}) \quad (14)$$

The global irradiation in one day is given by relation (15):

$$G_{tot} = \int_{HLS}^{HCS} I_g(t) dt \quad (15)$$

##### Specific Cooling Power (SCP)

The specific cooling capacity also called "Specific Cooling Power (SCP)" is the amount of cold produced per unit mass of adsorbent. It is given by the formula (16) below:

$$SCP = \frac{Q_{evapo}}{m_a \times t_{cycle}} \quad (16)$$

$t_{cycle}$  is the duration of a system operating cycle,  $m_a$  is the mass of adsorbent contained in the adsorber.

##### Climate data

In order to get closer to the actual operating conditions and to obtain near-real-life model performances, sunshine and ambient temperature were measured during a handling session on the adsorption solar refrigerator using the silicagel-water couple. This device is at the disposal of the Institute of Research in Applied Sciences and Technologies (IRSAT), located in the city of Ouagadougou (latitude :12°21'56N; longitude : -1°32'10). The manipulation session was held from 10/04/2016 to 13/04/2016. These climatic data will be implemented in the calculation program on the MATLAB software.

##### Resolution method

The system (S) consists of nonlinear differential equations with variable coefficients. To solve it, we first reduce to two equations in T (t) by eliminating equation (3) by substitution. Thus, the new system, after discretization in finite elements, can be written in the form of a tridiagonal system as follows :

$$aT(i-1) + bT(i) + cT(i+1) = d \quad (17)$$

Where,

$a=0$	$b = C_2 + \frac{A_2}{\Delta t} - C_3 \frac{m_a Q_{\text{adsorbt}}}{A_3 \Delta t}$	$c = \frac{A_2}{\Delta t} - C_3 \frac{m_a Q_{\text{adsorbt}}}{A_3 \Delta t}$	$d = B_2 I_g(i) + C_2 T_v(i) - \frac{m_a B_3 Q_{\text{adsorbt}}}{C_3}$
-------	--	--	--

## RESULTS AND DISCUSSION

The results that we present in this section have been obtained based on the considerations of the values of the following parameters and the operating conditions given by Table 1:

**Table 1: Parameter values and operating conditions**

Name	Symbol	Value	Unit
Wind speed	$V_{\text{vent}}$	2.7	m/s
transmissivity	$\tau_v$	0.9	
Emissivity of the glass	$\mathcal{E}_v$	0.88	
Height of the gap between the glass and the adsorber	d	0.05	m
Specific wall heat of the adsorber	$C_{pm}$	380	J/kgK
Absorption coefficient of the wall of the adsorber	$\alpha_{pm}$	0.8	
Emissivity of the wall of the adsorber	$\mathcal{E}_{pm}$	0.1	
Mass of adsorbent	$m_a$	10	kG
Effective thermal conductivity of the adsorbent	$\lambda_{eq}$	0.21	W/mK
Specific heat of the adsorbent	$C_{pa}$	1040	J/kgK
Maximum adsorption capacity	$\omega_o$	0.37	kG/kg
Constants of Dubinin-Astakhov	D ; n	1.8e-7 ; 2	
Condensation temperature	$T_c$	30	°C
Evaporation temperature	$T_e$	5	°C

### Transient behavior of adsorber collector state variables

Figure 4.a) shows the evolution of temperatures and sunshine and 4.b) the evolution of the pressure as a function of the operating time of the system. The sunshine and ambient temperature curves are obtained from the experimental values recorded during the day of 11/04/2016 on the IRSAT solar fridge. These values have been implemented in the MATLAB code. Simulations of the adsorbed mass of refrigerant and the pressure of the reaction medium are made by fixing the condenser and evaporator temperatures respectively at  $T_c = 30^\circ \text{C}$  and  $T_e = 5^\circ \text{C}$ . At sunrise, the temperature of the adsorber is almost equal to that of the ambient. As the time goes on, the adsorber overheats proportionally to solar radiation. This heating continues until the solar flux reaches its maximum value. For the day of 11/04/2016 this maximum value is  $1120 \text{ W} / \text{m}^2$  at the turn of 1.00 PM. At the same time, the recorded outdoor temperature reached  $36^\circ \text{C}$ . The temperature of the reaction medium reached a peak of  $94^\circ \text{C}$  while that of the glass is  $68.4^\circ \text{C}$ . Figure 5 illustrates these phenomena well. Indeed, the more the day is sunny, the higher the temperature inside the collector is improved. Just after these peaks, the solar flux decreases and the cooling of the adsorber begins and continues until the temperature is equal to the ambient temperature. The temperature threshold of the adsorbent bed is the regeneration temperature ( $T_g$ ), the temperature from which the adsorbate vapor desorption is finished. Numerical studies carried out by C. Wassila (2008) and K. Amadou et al (2016) on solar adsorption refrigeration systems operating with several adsorbent / adsorbate pairs, have shown that the highest  $T_g$  values make it possible to improve system performance. For the zeolite / water pair, the coefficient of thermal performance is between 0.4 and 0.47 when  $T_g$  is between  $87^\circ \text{C}$  and  $107^\circ \text{C}$  with  $T_a = 30^\circ \text{C}$ ,  $T_c = 30^\circ \text{C}$  and  $T_e = 5^\circ \text{C}$  (2008). Figure 6 also shows the time variation curves of the adsorbent bed temperature for different days of operation. It is noted that these curves have the same pace except that the temperature peaks vary from one day to another and are not reached at the same time of the day. This can be explained by the difference in solar flux received on the collector surface.

Furthermore, the pressure curve of the reaction medium (Figure 4 ; right column) has the same pace as the recorded daily solar flux. During the heating and cooling phases of the adsorber, the evolution of the pressure follows the same logic as the temperature. The maximums are reached from ten (10) hours. The translation of the second phase of the thermodynamic ideal cycle of the system during which the temperature increases with the heating while the pressure remains constant is clearly observed (Konfe, 2016). This phase is between ten (10) hours and fifteen (15) hours. At the start of heating and at the end of cooling, the minimum values are obtained which are close to 0.04 bar and 0.05 bar. The maximum pressure values are less than 0.55 bar. These extreme values are confirmed by the results of the study conducted by (Liu, 2005). Studies conducted by other authors (Wassila, 2008; Mimet, 1991) on different solar collector configurations using other couples, have obtained the same results on the behavior of the pressure in the reaction medium. Figure 6.a compares the amount of cold with instantaneous solar irradiation. There is an increase in the amount of cold produced in proportion to this irradiation. This can be justified from

Equation (14). Figure 6.b shows the changes in the refrigerant concentration in the reaction medium. The temperature evolution of the adsorber is inversely proportional to the change in concentration of the adsorbate in the adsorbent bed during the four phases of the operating cycle. During the heating phases, a decrease in the mass of water trapped in the zeolite is observed and during the cooling phases the remarks are reversed. The decrease in mass is explained by the fact that the rise in temperature and pressure in the adsorber causes desorption of water vapor by the adsorbent. And during the cooling of the adsorber, there is adsorption of liquid water by the adsorbent accompanied by the production of cold vaporization. It is important to note that Figure 6.b indicates that at the end of the desorption, some adsorbate (water) still remain trapped in the adsorbent (zeolite). This decreases the amount of refrigerant to be used in the next cycle and at the same time helps to reduce the cooling capacity compared to that of the previous cycle.

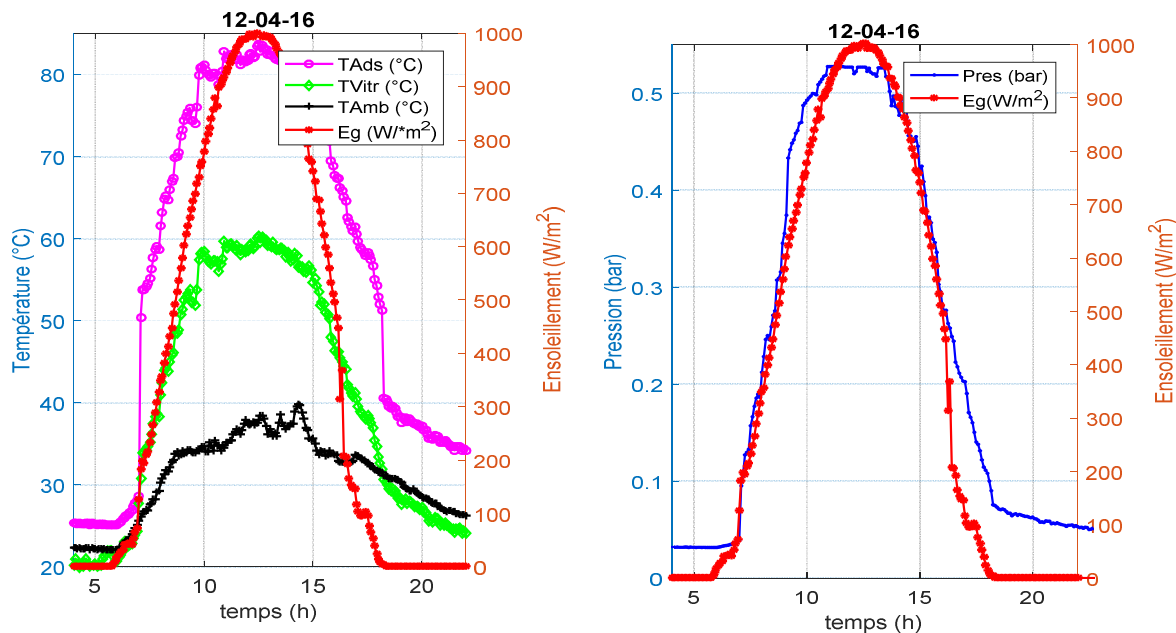


Fig.4:Curves of temperature variation, sunshine (a) and pressure (b) during the day of 12/04/2016

### Performance evaluation

**Effect of solar irradiation:** Figure 7 shows both the influence of solar irradiation recorded on April 12, on the amount of cold produced at the evaporator and on the solar coefficient of performance of the collector. There is a proportional change in the amount of cold produced with the energy received. In addition, the solar performance coefficient (COPs) hardly changes during the cycle. This is justified by the fact that the COPs can be defined as the coefficient of proportionality between the amount of cold produced at the evaporator and the energy received at the surface of the collector (according to equation 13).

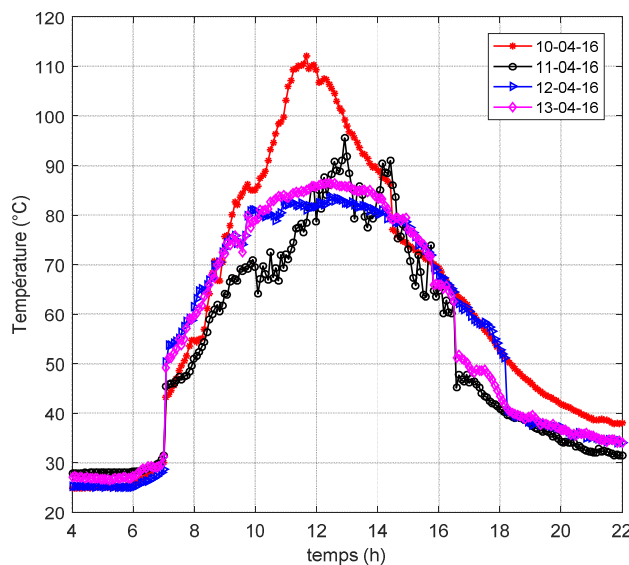


Fig. 5. Temperature variation curves of the adsorber corresponding to the sun from 10/04/16 to 13/04/16

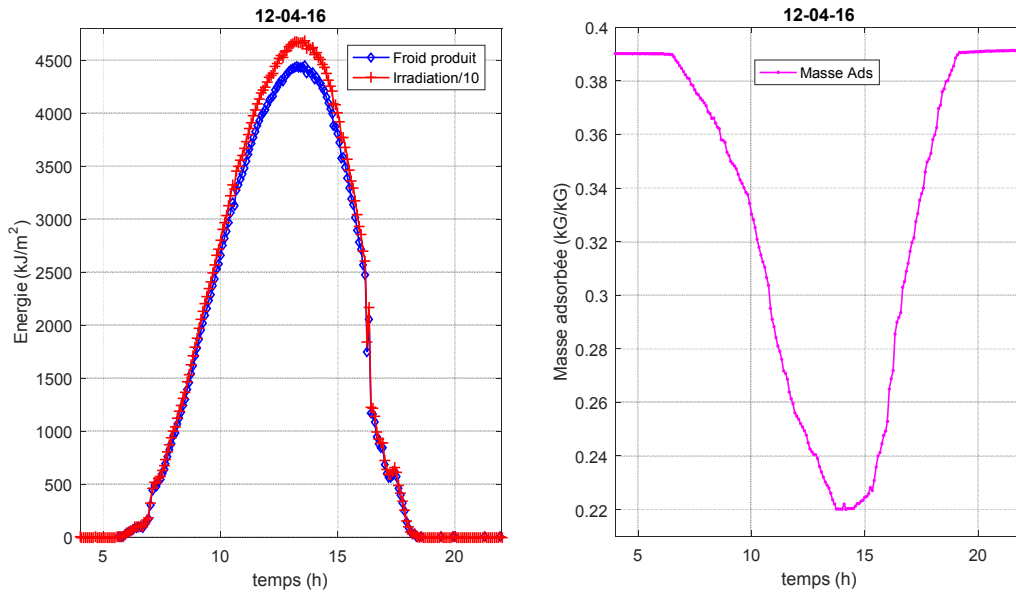


Fig. 6. Irradiation variation curves, cold produced and adsorbed mass during the day of 12/04/2016

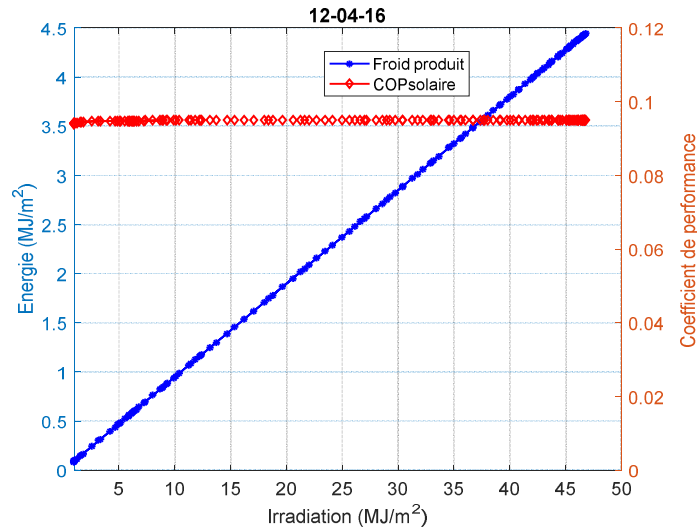


Figure 7. Curves of variation of cold produced and the coefficient of solar performance during the day of 12/04/2016

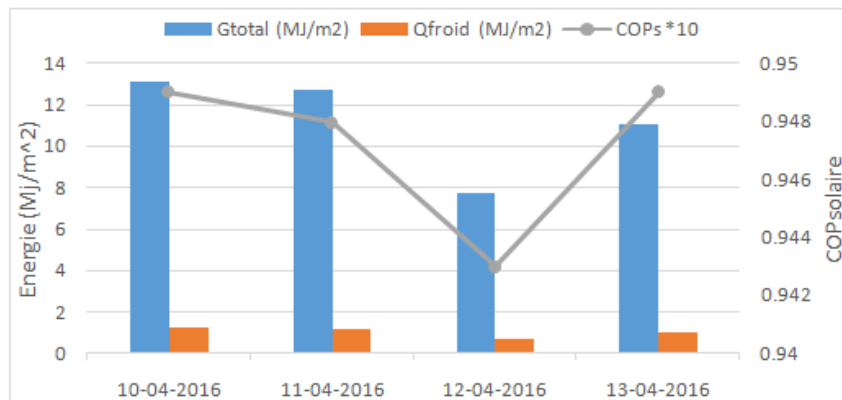


Fig. 8. Influence of irradiation on the solar coefficient of performance

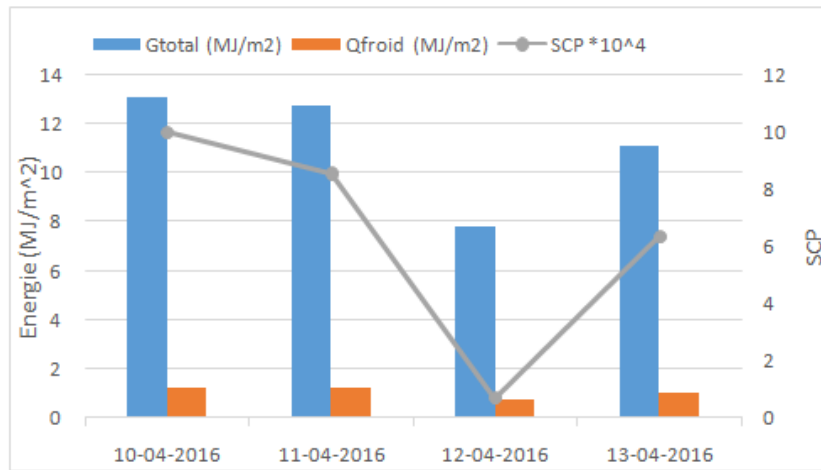


Fig. 9. Influence of irradiation on cooling capacity (SCP)

During an operating cycle, the COPs remain constant regardless of the quality of solar radiation received at the surface of the collector. To observe then the influence of the solar flux on the COPs, we present at the level of Figure 8, the irradiation values recorded every day for four days (from 10/4/16 to 13/04/16). These values made it possible to calculate the quantity of cold and the COPs corresponding to each twenty-four hour cycle. The more stored energy is important the higher the solar COPs. Indeed, the amount of cold produced increases with the irradiation (according to figure 7). However, the COPs vary with the amount of cold drawn off at the evaporator, hence this result. Studies conducted in this way by (Wassila, 2008; Konfe, 2016) have led to similar results. Fig. 9 shows the influence of the irradiation on the cooling capacity of the system during the days from 10/04/16 to 13/04/16. Remarks made in fig. 8 are also observed in this figure.

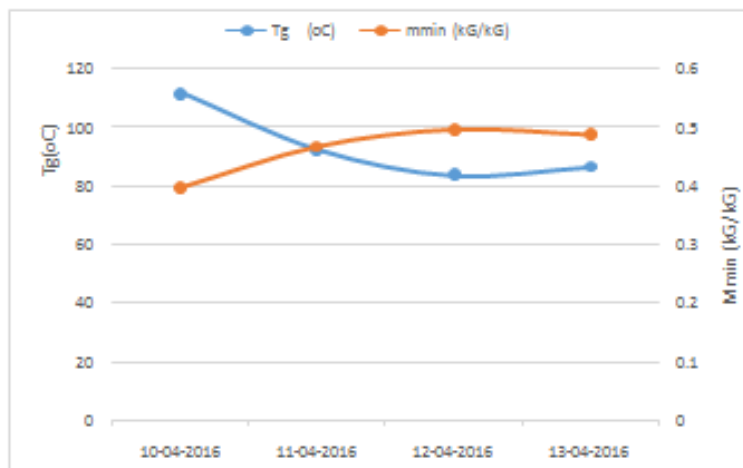


Figure 10. Influence of the regeneration temperature on the desorbed mass



Figure 11. Influence of the regeneration temperature on the amount of cold produced

**Effect of regeneration temperature :** Figures 10 and 11 respectively show the influence of the regeneration temperature on the desorbed adsorbate mass during the desorption-condensation phase. It is found that the concentration of the adsorbate in the adsorbent is even smaller than when the regeneration temperature is high. It is the same for the amount of cold produced at the evaporator. As a result, the improvement in the extreme value of the temperature of the adsorber causes a decrease in the mass of water contained in the adsorbent at the end of the desorption phase. This allows at the same time to improve the amount of cold drawn to the evaporator. For this, O.S. Headly (1994) has shown that the use of CPC concentrators as a collector makes it possible to increase the values of the regeneration temperature. Other authors (Saeung, 2005) have shown that the use of a vacuum pump between the reactor and the condenser in the case of a hybrid refrigerator makes it possible to increase the recovery of the desorbed mass by lowering the pressure of the reactor.

## Conclusion

In this work, it was about studying in on one hand, the distribution of the state variables within the adsorber-collector of a solar adsorption refrigerator using the zeolite-water pair and on the other hand their influences on the parameters that characterize the performance of the system. The sun and ambient temperature values recorded on the IRSAT sensor from 11/04/16 to 13/04/16 have enabled us to obtain results on our model for operation in the real climate conditions of the city of Ouagadougou. The results obtained show that for maximum sunshine values between 900 and 1100 W/m<sup>2</sup> and maximum outside temperatures sometimes reaches 41 °C, the temperature of the reaction medium reaches peaks or maximum regeneration temperatures (T<sub>g</sub>) ranges from 88 °C at 110 °C, the pressure in the reaction medium varies between 0.04 and 0.55 bar. The desorbed adsorbate mass produces a cold amount of up to 1.2438 MJ/m<sup>2</sup> over one cycle. The determination of these quantities made it possible to calculate the solar performance coefficient (COPs) and the cooling capacity (SCP) of the system. These values vary proportionally with the amount of cold produced and the desorbed mass which are directly proportional to the regeneration temperature (T<sub>g</sub>) and solar irradiation. In sum, this study shows that in order to improve the performance of the system, it is important to take into account the evolution of the state variables such as the temperature of the adsorbent bed, the sunshine, the pressure, the refrigerant mass desorbed at the end of the desorption-condensation phase.

## REFERENCES

- Adell, A. 1984. Réfrigération solaire à adsorption solide : choix du meilleur couple d'adsorption. *Révue de Physique Appliquée*, 19(12) :1005-1011. ISSN 0035-1687. doi : 10.1051/rphysap : 0198400190120100500
- Al Mers, A., Azzabakh, A., Mimet, A. and El Kalkha. H. 2006. Optimal design study of cylindrical finned reactor for solar adsorption cooling machine working with activated carbon- ammoniac pair. *Applied Thermal Engineering*, 26(16) : 1866-1875. ISSN 1359-4311. DOI : <http://dx.doi.org/10.1016/j.applthermaleng.2006.01.021>.
- Bing Xue, Xiangrui Meng, Koichi Nakaso, and Jun Fukai. 2015. Dynamic studyof steam generation from low-grade waste heat in a zeolithe-water adsorption heat pump. *Applied Thermal Engineering*. September 88 : 1542-1547. DOI : 10.1016/j.applthermaleng.2014.11.050
- Boubakri, A., Arsalane, M., Yous, B., Ali-Moussa, L., Pons, M., Meunier, F. and Guilleminot. J.J. 1992. Experimental study of adsorptive solar powered ice makers in Agadir (Morocco)-1. Performance in actual site. *Renewable Energy*, february 2(1) :7-13. ISSN 0960-1481. doi : 10.1016/0960-1481(92)90054-7.
- DELPORTE Loïc, DUBUISSON Julie, FOUREZ Antonin, URBAIN Fanny, WERTH Annette Codepo, 2008/09. Développement d'un prototype de frigo solaire destiné à la conservation des vaccins, Projet, Université Libre de Bruxelles .
- El Amers. A. 2002. Etude du transfert de chaleur et de masse dans un lit fixe de charbon actif réagissant par adsorption avec l'ammoniac application à la modélisation d'une machine frigorifique solaire. Thèse de Doctorat, Université de Tétouan Maroc.
- Headly, O. S., Kothdiwala, A. F. and Mcdoom, I. A. 1994. Charcoal/methanol adsorption refrigerator powered by a compound parabolic concentrating solar collector. *Solar energy*, Vol. 53, pp 191-197.
- Hilbrand, C., Dind, P., Pons, M., Buchter. F. A. 2004. New solar powered adsorption refrigerator with high performance. *Solar Energy*. 77(3) :311-318. Doi : 10.1016/j.solener.2004.05.007.
- KONFE Amadou. 2017. Etude Thermique et Conception d'un réfrigérateur solaire à adsorption. Thèse de Doctorat. Université Ouaga I Pr Joseph KI ZERBO. Burkina Faso.
- Konfe, A., Kam, S., Ousmane M. and Bathiebo. D.J. 2016. *Comparative thermodynamic study of five couples used in solar cooling with adsorption by simulation. British Journal of Applied Sciences & Technology*. ;17(2) :1-17. DOI : 10.9734/BJAST/2016/28554
- Krache. L. 1996. Contribution à l'étude théorique d'un réfrigérateur solaire à adsorption utilisant le couple zéolithe 13X-eau. PhD thesis, Université Constantine.
- Leite, A. P. F., Daguene, M. 2000. Performance of a new solid adsorption ice maker with solar energy regeneration, *Energy. Convers. Manag.*, Vol. 41, pp 1625 - 1647.
- Leite, A. P. F., Daguene, M. 2000. Performance of a new solid adsorption ice maker with solar energy regeneration, *Energy. Convers. Manag.*, Vol. 41, pp 1625 - 1647.
- Lemmin F, Buret-Bahraoui J, Pons M, Meunier F. 1992. Simulion des perfomances d'un réfrigérateur solaire à adsorption : 1. Comparaison des performances pour deux types de charbon actifs. *International Journal of Refrigeration*. 15(3) :159-167. Doi : 10.1016/0140-7007(92)90006-G.
- Liu et Y., Leong, K. C. 2005. The effect of operating conditions on the performance of the zeolithe/ water adsorption cooling systems, *Applied thermal engineering* 25.

- Meunier, F. 1988. Theoretical performance of solid adsorbent cascading using the zeolithe/water and active carbon/methanol pairs: four cases studies, heat recov. Sys.; 6(6) : 491- 498.
- Meunier, F. 1986. Theoretical performances of solid adsorbent cascading cycles using the zeolithe-water and active carbon-methanol pairs : four case studies. Journal of heatrecovery systems. 6(6) :491-498.
- Mimet, A. 1991. Etude théorique et expérimentale d'une machine frigorifique à adsorption d'ammoniac sur charbon actif. PhD thesis, FPMS Mons, Belgique, FPMS,
- Mohammed Abdel bassat Slasli. 2002. Modélisation de l'adsorption par les charbons microporeux : Approche théorique et expérimentale. PhD Thesis, Université de Neuchâtel- Faculté des Sciences.
- Phillipe, D., Hildbrand, C., Cherbuin, O., Mayor, J. 2005. La réfrigération solaire à adsorption. HES-CO : projet Gerbert RufStiftung. Yverdon-les-Bains, Suisse
- Pons M. and Ph. Grenier, 1986. A phenomenological adsorption equilibrium law extracted from experimental and theoretical considerations applied to the Activated Carbon + Methanol pair, Carbon, 24-5, pp 615-625.
- Rouquerol, F. 1982. Textures des solides poreux ou divisés. Technique de l'ingénieur, P 3645, PP 1-14.
- Saeung, S., Boussechain, R. Feidt, M. 2005. étude du comportement d'une machine à adsorption, rapport final interne- PR 2.9, contribution de LEMTA, Université de Nancy.
- Sun L. M and Meunier, F. 2003. Adsorption : Aspects théoriques. Technique de l'ingénieur. J 2730 :1-16.
- SUN, L. M. Meunier, F. 2003. Adsorption. Aspects théoriques, J 2 730 Techniques de l'Ingénieur, pp 1-20.
- Talu O. et al. Langmuir. J. Phys. Chem. 93.
- Trombe, F. F., M. 1956. Sur la production de froid à l'aide du rayonnement solaire. *Compte rendu hebdomadaire de l'Académie des Sciences p 242, 8.*
- Wassila. C. 2008. *Etude et analyse d'une machine frigorifique solaire à adsorption*, thèse de Doctorat, Université Mentouri Constantine, Algérie.
- ZOUBIR, B. 2007. Modélisation et étude de la faisabilité d'un réfrigérateur solaire à adsorption, Magistère.

\*\*\*\*\*